

**A High-Resolution Gamma-ray and Hard X-ray Spectrometer
for Solar Flare Observations in Max-91**

R. P. Lin, D. W. Curtis, P. Harvey, K. Hurley, J. H. Primbsch, D. M. Smith
Space Sciences Laboratory, University of California at Berkeley

R. M. Pelling, F. Duttweiler
CASS, University of California at San Diego

ABSTRACT

We describe a long duration balloon flight instrument for Max-91 designed to study the acceleration of >10 MeV ions and >15 keV electrons in solar flares through high resolution spectroscopy of the gamma-ray lines and hard X-ray and gamma-ray continuum. The instrument, HIREGS, consists of an array of high-purity, n-type coaxial germanium detectors (HPGe) cooled to $<90^\circ\text{K}$ and surrounded by a bismuth germanate (BGO) anticoincidence shield. It will cover the energy range 15 keV to 20 MeV with keV spectral resolution, sufficient for accurate measurement of all parameters of the expected gamma-ray lines with the exception of the neutron capture deuterium line. Electrical segmentation of the HPGe detector into a thin front segment and a thick rear segment, together with pulse-shape discrimination, provides optimal dynamic range and signal-to-background characteristics for flare measurements. Neutrons and gamma-rays up to $\sim 0.1-1$ GeV can be detected and identified with the combination of the HPGe detectors and rear BGO shield.

HIREGS is planned for long duration balloon flights (LDBF) for solar flare studies during Max-91. We describe the two exploratory LDBFs carried out at mid-latitudes in 1987-88, and discuss LDBFs in Antarctica, which could in principle provide 24 hour/day solar coverage and very long flight durations (20-30 days) because of minimal ballast requirements.

Introduction

High resolution spectroscopy of flare gamma-ray line and hard X-ray and gamma-ray continuum emission can provide a qualitatively new window on flare particle acceleration processes. This is because essentially all the nuclear gamma-ray lines produced by the energetic ions, and many of the important features of the hard X-ray continuum produced by the energetic electrons, are unresolved by present spacecraft detectors (Figure 1). High resolution measurements from ~ 10 keV to ≥ 20 MeV are required for:

- 1) Nuclear line spectroscopy, including determination of line shapes and asymmetries, to provide detailed information on the shape of the energy spectrum and angular distribution of the accelerated ions.¹
- 2) Flare hard X-ray continuum spectroscopy to provide the detailed shape of the energy spectrum of the accelerated electrons which very likely carry a large fraction of the total flare energy.² High resolution is required to resolve the steep spectrum of the emission from the high temperature "superhot" plasmas³ in the flare and to identify and resolve the sharp breaks⁴ in the accelerated electron spectrum. These features appear to be critical clues to the acceleration mechanism.
- 3) Very high sensitivity measurements of the narrow neutron capture deuterium line at 2.223 MeV to determine whether even small flares can accelerate ions to > 10 MeV energy.⁵
- 4) Resolution of the many expected nuclear gamma-ray lines to provide a powerful new method of obtaining solar elemental abundances.⁶
- 5) Determination of the shape and temporal evolution of the positron annihilation line at 511 keV to give information on the temperature and density of the annihilation region.⁷

With high sensitivity measurements the temporal evolution of the accelerated ions and electrons can be closely followed, and the role of electron acceleration in very small transient releases of energy, i.e., microflares,⁸ and their relationship to coronal heating,

can be explored.

Below we describe the design for a High Resolution Gamma-Ray and Hard X-ray Spectrometer (HIREGS). HIREGS cleanly separates the ≤ 200 keV hard X-ray region from the gamma-ray line region (0.4–20 MeV) so the high spectral resolution needed for line measurements can be maintained even in the presence of the very intense [$\geq 10^4$ (cm² sec)⁻¹ above 10 keV] flare hard X-ray fluxes.

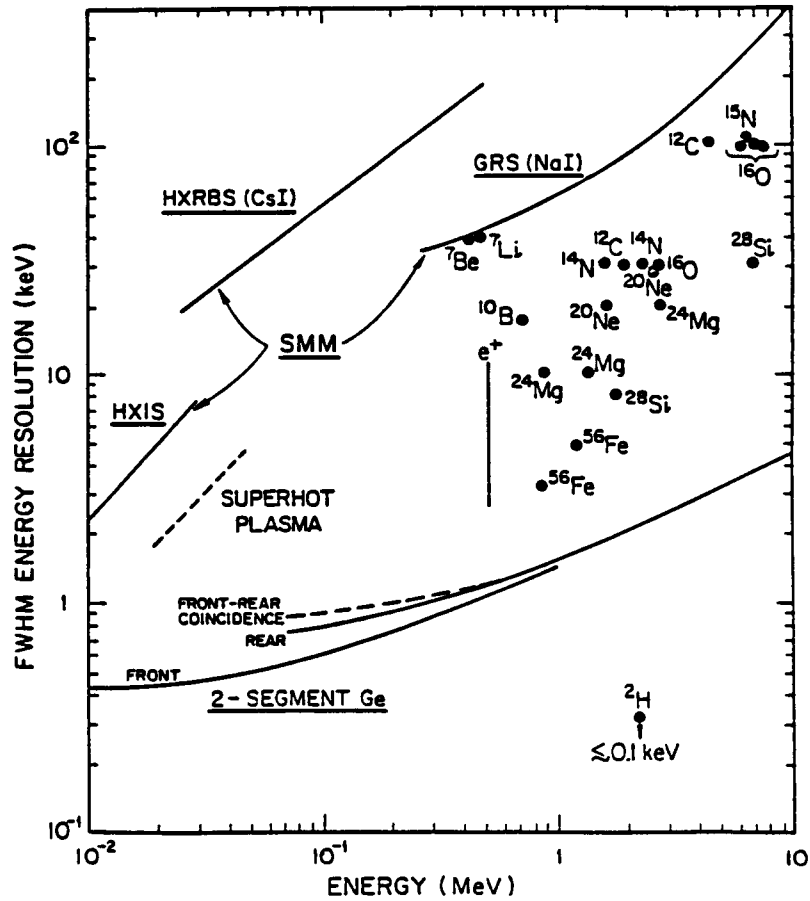


Fig. 1. The spectral resolution of the HIREGS 2-segment HPGe detectors is compared with that of the hard X-ray and gamma-ray instruments on SMM. The typical line widths expected for gamma-rays in solar flares are shown, as well as the resolution required to resolve the steep super-hot thermal component (dashed line).

Instrument Description

HIREGS consists of an array of 12 dual-segment, high-purity germanium (HPGe) detectors in a BGO scintillator annulus and back shield/detector assembly (Figure 2). The HPGe detectors are contained in a cryostat and cooled to an operating temperature of 90°K with liquid nitrogen. Table I gives the instrument parameters.

Segmented HPGe Detectors

The closed-end HPGe detectors are fabricated from n-type material, 6.5 cm in diameter and 6.5 cm thick, and are operated in the reverse bias mode, i.e., the holes are collected by the outside electrode.

Each detector has multiple collecting electrodes which divide it into two distinct volumes, or segments, according to the electric field pattern (Figure 3). In the central 1.0 cm diameter hole which extends to within ~8 mm of the top, two separate contacts are provided.¹⁰ The top contact collects charge from the upper 1 cm segment of the detector, and the long lower contact collects charge from the bottom ~5.5 cm coaxial segment. The curved outer surface and top surfaces are implanted with boron to make a very thin (~0.3 micron) window for X-rays.

The top segment alone is used at low energies (≤ 200 keV) where photoelectric absorption dominates (Figure 4). Photons are absorbed in the top ~1 cm segment, while Compton scattered photons and detector background are rejected by anticoincidence with the adjacent bottom segment of the detector. Therefore, this mode has the excellent background rejection properties of a phoswich type scintillation counter.¹¹

Higher energy (≥ 200 keV) photons are detected primarily in the thick bottom segment alone mode, with a smaller fraction also detected via top-bottom coincidences (Figure 4). The bottom segment is shielded by the top segment from low energy, $\leq 10^2$ keV protons. Even in the largest flares the peak count rates of the bottom segment is $\leq 2 \times 10^4$ c/s per detector. Each detector has independent signal paths for the front and rear segments as indicated in Figure 3. Each signal path includes a cooled FET wide bandwidth charge sensitive preamplifier, followed by dual shaping amplifiers.¹² A slow shaper-amplifier (~10 μ s time constant) is used for pulse height analysis, and a fast shaper-amplifier-discriminator (~100 ns) supplies fast pulses for coincidence. pileup

rejection, timing, and rate accumulations. The pile-up rejection system allows operation at rates up to $5 \times 10^4 \text{ s}^{-1}$ per detector without resolution degradation.

Table II shows that in a flare the size of the 27 April 1981 gamma-ray flare,¹³ several hundred to a couple thousand counts would be obtained by HIREGS in each of a dozen major lines (including four lines of Fe). Flare bremsstrahlung continuum will usually dominate the detector background, leading to line-to-continuum ratios of $I/c \approx 1$ to 10, except for the broad Li-Be combined lines where $I/c \approx 0.2$. These lines will be detected at ~ 10 – 60σ 's significance, permitting line shapes, asymmetries, etc. to be accurately determined. Even for a flare with line fluences more than 30 times smaller, most of these lines could be detected at the 3σ level if the I/c remained the same. For detection of narrow lines HIREGS is ~ 5 – 10 times as sensitive as the SMM GRS instrument.

The most sensitive indicator of ion acceleration is the narrow nuclear line of neutron capture deuterium at 2.223 MeV, which is delayed from the impulsive phase by the thermalization time for the neutrons. HIREGS can detect at 3σ significance a 2.223 MeV line fluence $\geq 10^3$ times smaller than the 4 August 72 event. If all flares accelerate ions to tens of MeV energy and the gamma-ray emission scales as the microwave burst intensity, then ~ 10 – 15 flares should be detected per month in the 2.223 MeV line near solar maximum.

Good background rejection is important for the 511 keV positron annihilation and the 2.223 MeV neutron capture deuterium line, which usually lasts well past the impulsive phase. Also SMM observations show that following the impulsive phase there is a delayed phase in some (perhaps many) flares which is dominated by nuclear emissions.¹⁴ The segmented HPGe detector provides the basic configuration for powerful background rejection techniques in the gamma-ray line region from a few hundred keV to several MeV (see ^{15,16} for details).

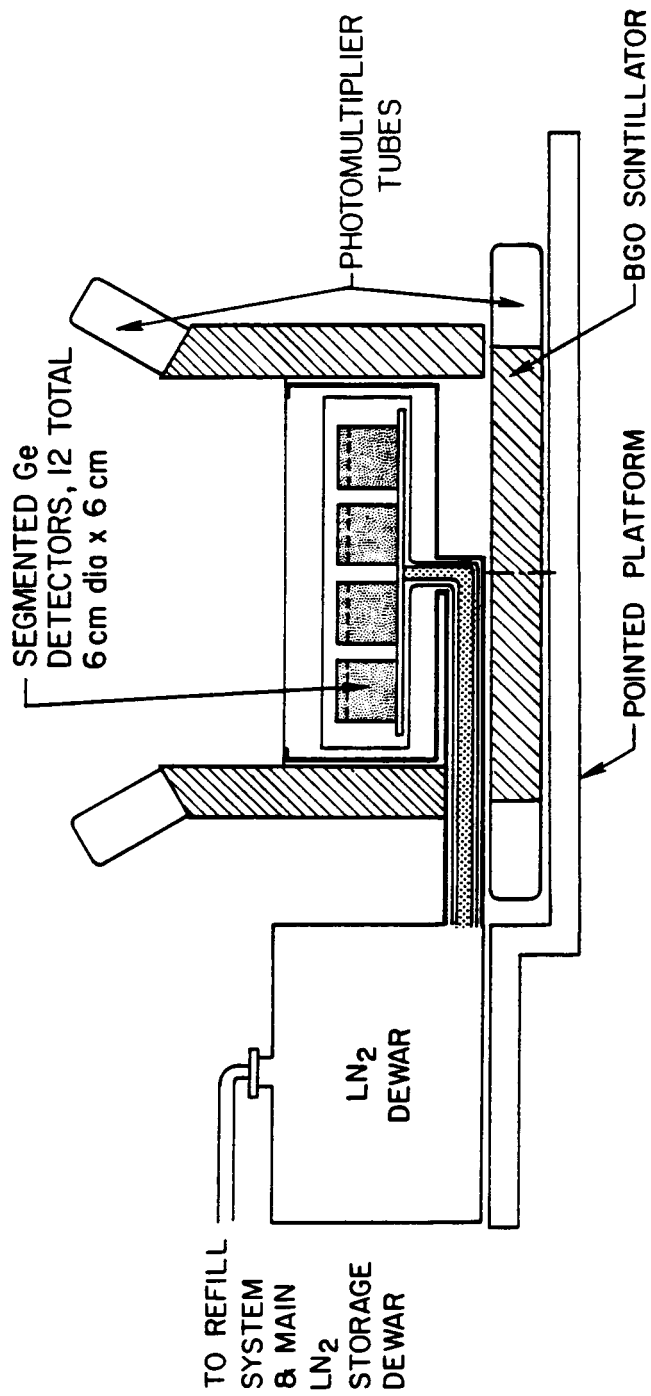


Fig. 2. Schematic of HIREGS instrument.

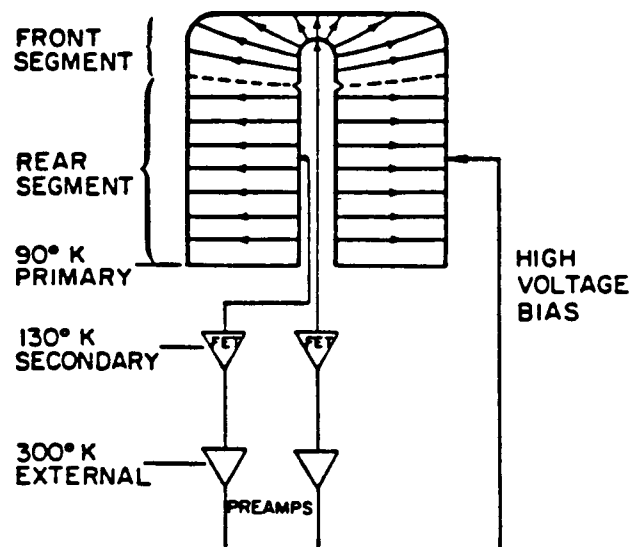


Fig. 3. Schematic of a dual-segment HPGe detector.

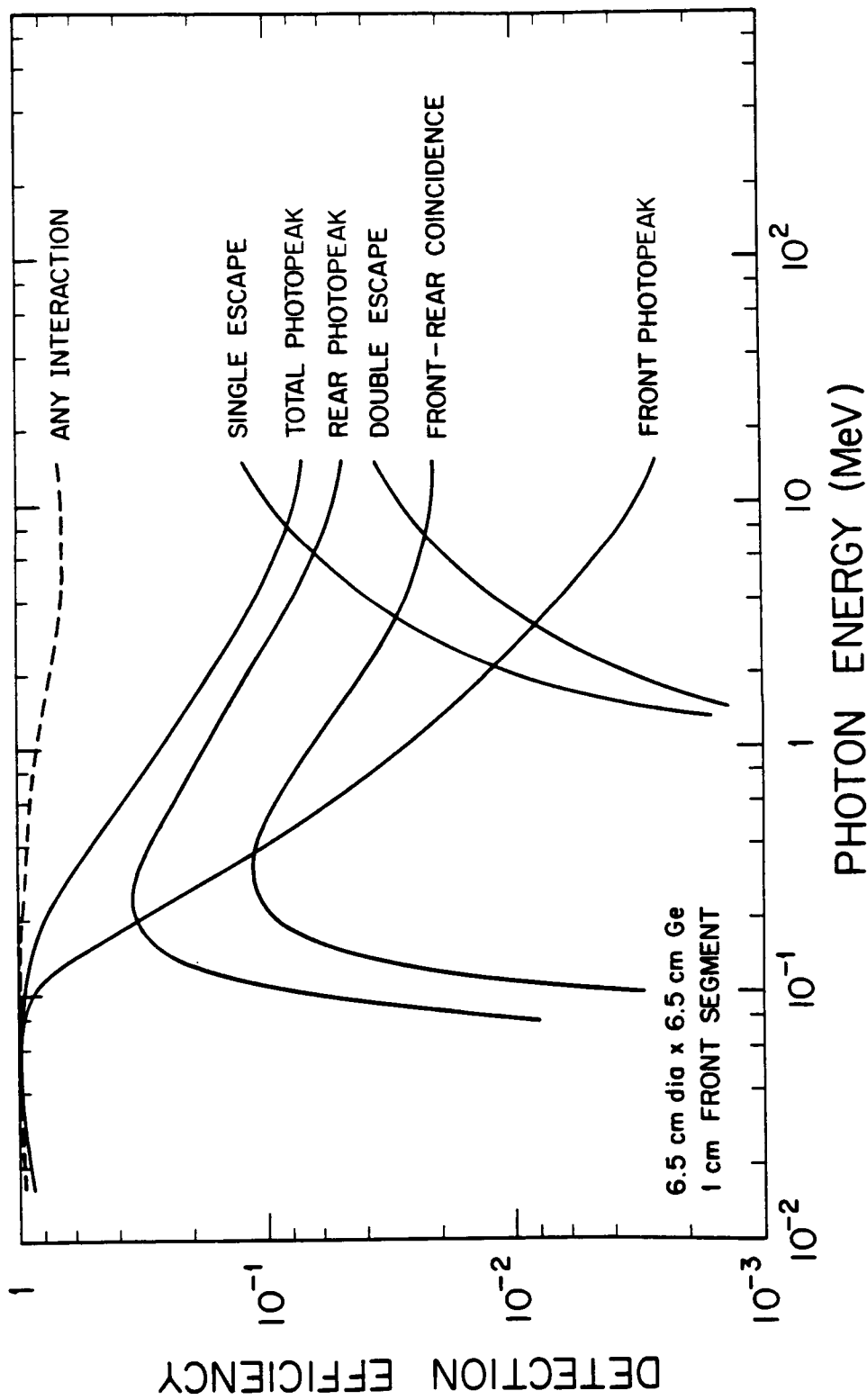


Fig. 4. The photopeak efficiency for the top segment and bottom segment of the HPGe detector is shown here for different modes.

Table I. HIREGS Instrument Parameters

Energy range	Gamma-rays and hard X-rays	10 keV to 20 MeV (high-resolution HPGe)
Energy resolution		0.6 to 5 keV FWHM (high-resolution HPGe)
Total detector area		400 cm ² HPGe
Field of view		120° FWHM
Shields		5-cm-thick BGO on sides and rear
Germanium detector cooling		~90°K for 20 days with liquid nitrogen

Table II. Solar Flare Gamma-Ray Lines

Line Energy (MeV)	Excited Nucleus	FWHM (keV)	Fluences at Earth in FWHM		Counts in HIREGS (1000 s)			HIREGS 3σ line sensitivity fluence ph/cm ² (10 ² /10 ² s)
			Lines	Flare Continuum (ph/cm ²)	Line	Flare Continuum	Detector Background	
Prompt Lines								
~0.45	⁷ Li, ⁷ Be	62	20	105	3.7×10 ³	1.1×10 ⁴	1.7×10 ³	0.67/0.2
0.847	⁵⁶ Fe	4.5	5	2	630	250	40	0.15/0.05
0.931	⁵⁶ Fe	5	2	2	230	230	35	0.15/0.05
1.238	⁵⁶ Fe	9	2.5	2	250	200	35	0.2/0.06
1.317	⁵⁶ Fe	13	2.5	2	240	190	45	0.2/0.06
1.369	²⁴ Mg	18	7.5	3	690	280	55	0.25/0.08
1.634	²⁰ Ne	23	13	2.5	1.1×10 ³	200	45	0.25/0.08
1.779	²⁸ Si	25	8	2	630	180	45	0.25/0.08
2.313	¹⁴ N	54	6	3	410	205	50	0.3/0.1
4.438	¹² C	115	10	1.5	510	80	20	0.25/0.08
6.129	¹⁶ O	120	10	1	440	44	10	0.2/0.06
Delayed Lines								
0.511	e ⁺	2-10	25	—	4.3×10 ³	—	44-220	~0.25/~0.12
2.223	² H	3(0.1)*	60(4.3)*	—	4×10 ³	—	3	0.1/0.05

* This line has an intrinsic width of ~0.1 keV, so the HIREGS instrument FWHM resolution (3 keV) is substituted. The 2.223 MeV fluence observed for the 27 April 1981 flare is highly attenuated because the flare is located near the limb; the value of 60 is for a comparable flare within ~70° of disk center.

Long Duration Balloon Flights

Long duration balloon flights (LDBF) offer an attractive way to obtain high energy measurements during the next solar maximum, since energetic photons and neutrons are able to penetrate the upper layers of the earth's atmosphere. Large, powerful instruments, up to ~3000 lbs. total payload weight, can be carried by the present standard 28.4 million cu. ft. balloons to altitudes of ~130,000 ft. (40 km). At that altitude there is less than 3 g/cm² of overlying atmosphere, so high quality hard X-ray and gamma-ray measurements down to ~15 keV are possible.

For standard zero-pressure balloons the temperature of the gas, and therefore the balloon altitude, is controlled by the radiation received from the Sun and the Earth. Thus the balloon is at high altitude during sunlight hours but drops during nighttime. If the balloon initially reaches a high daytime float altitude it will remain above the tropopause in its day-night excursions under normal conditions without ballast drops. Then, in this simple **R**adiation **C**ontrolled ballo**ON** (RACOON) mode,¹⁷ flight durations are limited only by balloon lifetime and gas losses (which can be offset by ballast drops). During the three-month summer season at mid-latitudes, strong stable zonal winds flow with high velocity approximately along latitudinal lines, so circumglobal LDBFs are feasible.

In 1983 a 15 million cubic ft. balloon with an ~1200 lb. payload, designed to search for solar flare neutrons, made a circumnavigation of the globe in the southern hemisphere in ~18 days.¹⁸ In 1987, two exploratory RACOON balloon flights were launched from Alice Springs, Australia. One payload carried a complement of hard X-ray and gamma-ray detectors, including both liquid-nitrogen cooled germanium detectors for high spectral resolution and large-area phoswich scintillation detectors for high sensitivity, for observations of microflares and flares from the sun.¹⁹ The standard, 28.4 million cubic ft., 0.8 mil polyethylene, zero-pressure balloon developed for normal short-duration flights was used. The payload was designed for automated continuous 24 hours/day operation with a solar cell power system, a pointing and navigation system, data and telemetry systems, etc.

The payload was launched at ~2100 UT February 9, 1987, from Alice Springs, Australia. Due to a malfunction of the ballast control system all 900 lbs of ballast were dropped at launch. The balloon thus flew as an unballasted RACOON for the entire flight. With the loss of ballast the ascent was extremely rapid (~1500 ft./min), and the balloon reached a float altitude of ~132,000 ft.—i.e., ~2000 ft. higher than normal. Some of the helium was vented, and perhaps some leaks developed from the stress of the rapid ascent.

Figure 5 shows the balloon altitude versus time. The daytime float altitude generally decreased throughout the flight. Preliminary analysis indicates that balloon lift decreased at a rate of ~2–3% per day, possibly from a small leak. The gas temperature, and therefore the float altitude, are determined primarily by the radiation the balloon receives from the sun and the earth. Cold storm clouds below the balloon are responsible for the sharp drops in altitude superimposed on the general long-term decrease. Ballast drops totaling ~15% (900 lbs) of the total balloon plus payload weight would have kept the daytime balloon float altitude near 130,000 ft. for the entire trip from Australia to Brazil.

The trajectory of the balloon is shown in Figure 6. The balloon started westward at an average rate of ~30° longitude per day (~130 km/hour), but slowed down as the balloon altitude decreased. The payload was commanded to cut down over Brazil after 12 days, and was recovered with relatively minor damage.

All the detectors, the experiment data system, and electronics appeared to have functioned perfectly. The data transmission to the GOES spacecraft appears to have been intermittent. Only ~10% of those data have been recovered. All of the data, however, were stored in the on-board VCR tape. Analysis of those data is underway.

In January-February 1988 two more 28.4 million cu. ft. balloons were flown from Alice Springs, Australia to Brazil. One payload contained germanium and scintillation detectors to search for gamma-ray lines and hard X-ray continuum from the new supernova 1987A. Again, the ballast system malfunctioned, but the balloon made it to Brazil after ~9 days.

Also in January, 1988, a 11.8 million cu. ft. balloon carrying a coaxial germanium detector system was launched from near McMurdo in Antarctica (latitude $\sim 78^\circ\text{S}$), again to search for gamma-ray lines from the new supernova 1987A. The balloon drifted very slowly along the 78° latitude line and the payload was cut down 65 hours later near Vostok, about 80° west of McMurdo, where the payload was recovered. Because of the 24-hour sunlight, the balloon lost less than 0.5% of its lift per day. Thus, in addition to the possibility of 24-hour observation per day, versus ~ 12 at mid-latitudes, much longer flights (perhaps 20–30 days) are feasible because much less ballast is needed.

In the Antarctic during the summer the sun will be at angles to the zenith of $\sim 67^\circ$. Thus, solar photons must traverse $\sim 7.7 \text{ g/cm}^2$ of atmosphere to reach a balloon instrument at a height of $\sim 130,000$ ft. (3 g/cm^2 overlying atmosphere). At mid-latitudes the overlying atmosphere (at the same altitude) is $\sim 3 \text{ g/cm}^2$ near noon but averaged over the full 12 hours/day of observing provides only $\sim 10\text{--}20\%$ better transmission of gamma-ray line energies than Antarctica (Figure 7). The difference rises to about a factor of two at hard X-ray energies, but of course photons are plentiful in that range.

The much longer flight durations and 24 hours/day observation times available for Antarctica very significantly increase the probabilities for detecting solar gamma-ray events. Clearly Antarctic balloon flight capabilities need to be developed for Max-91.

Table III summarizes the expected number of gamma-ray line and hard X-ray flare events for a typical mid-latitude, Australia to Brazil flight, and for a ~ 12 day circumnavigation flight around the south pole. Because of the low ballast requirements, two circumnavigations should be possible in a single flight, so that numbers in Table III for Australia could be doubled.

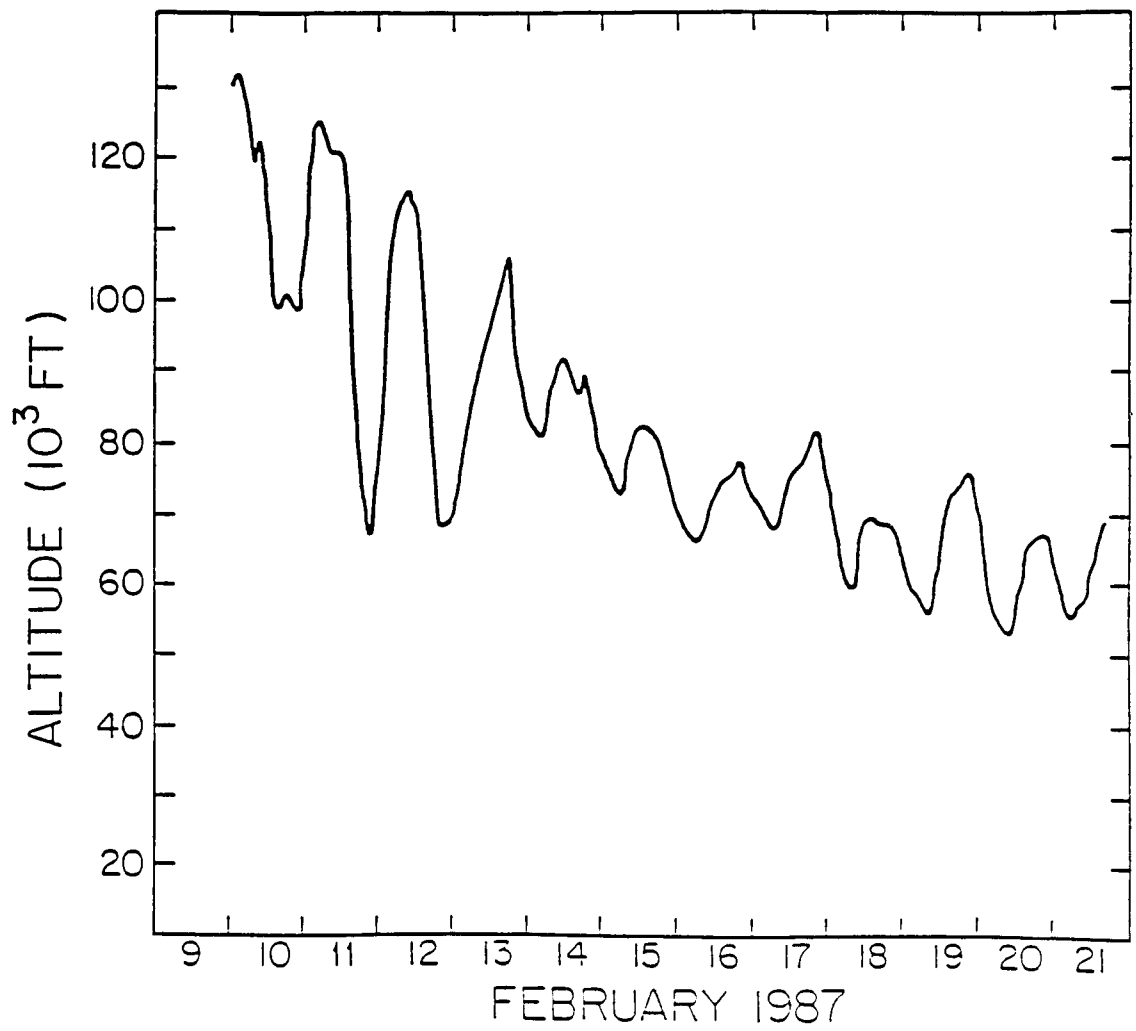


Fig. 5. Balloon altitude versus time (unballasted).

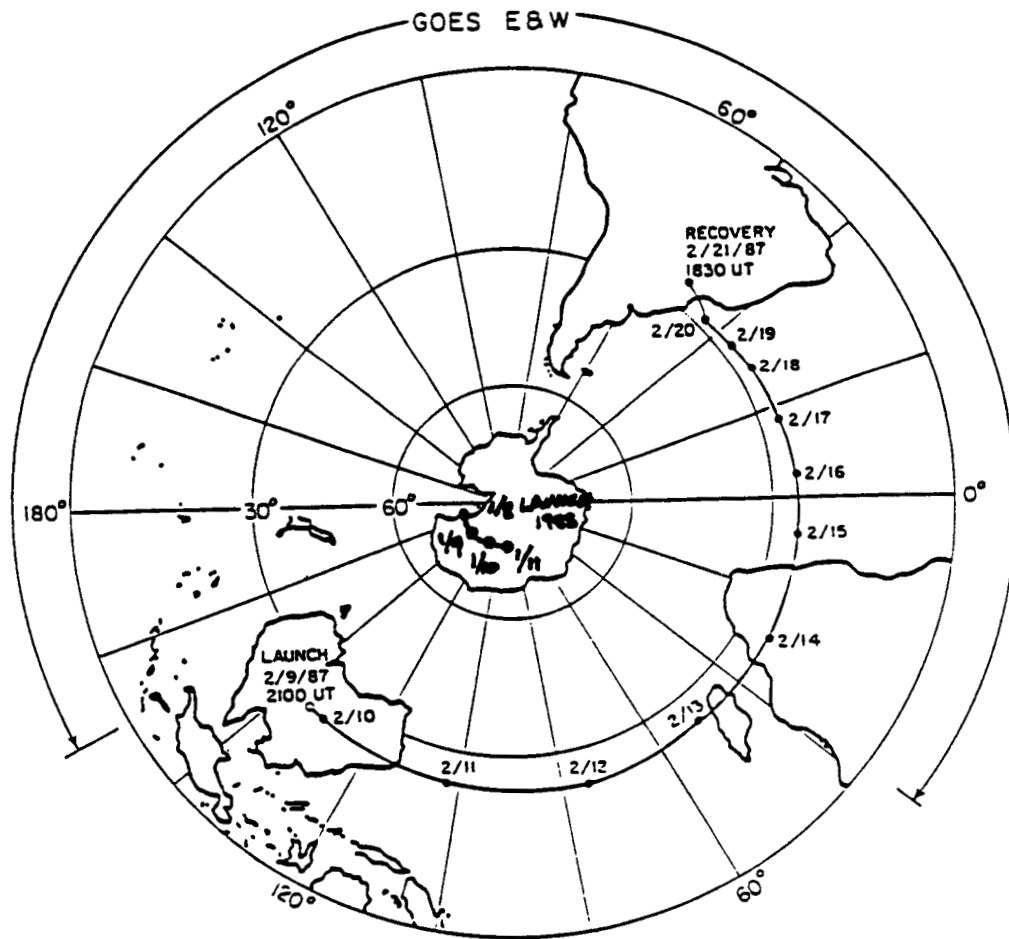


Fig. 6. Balloon trajectory from Australia to Brazil.

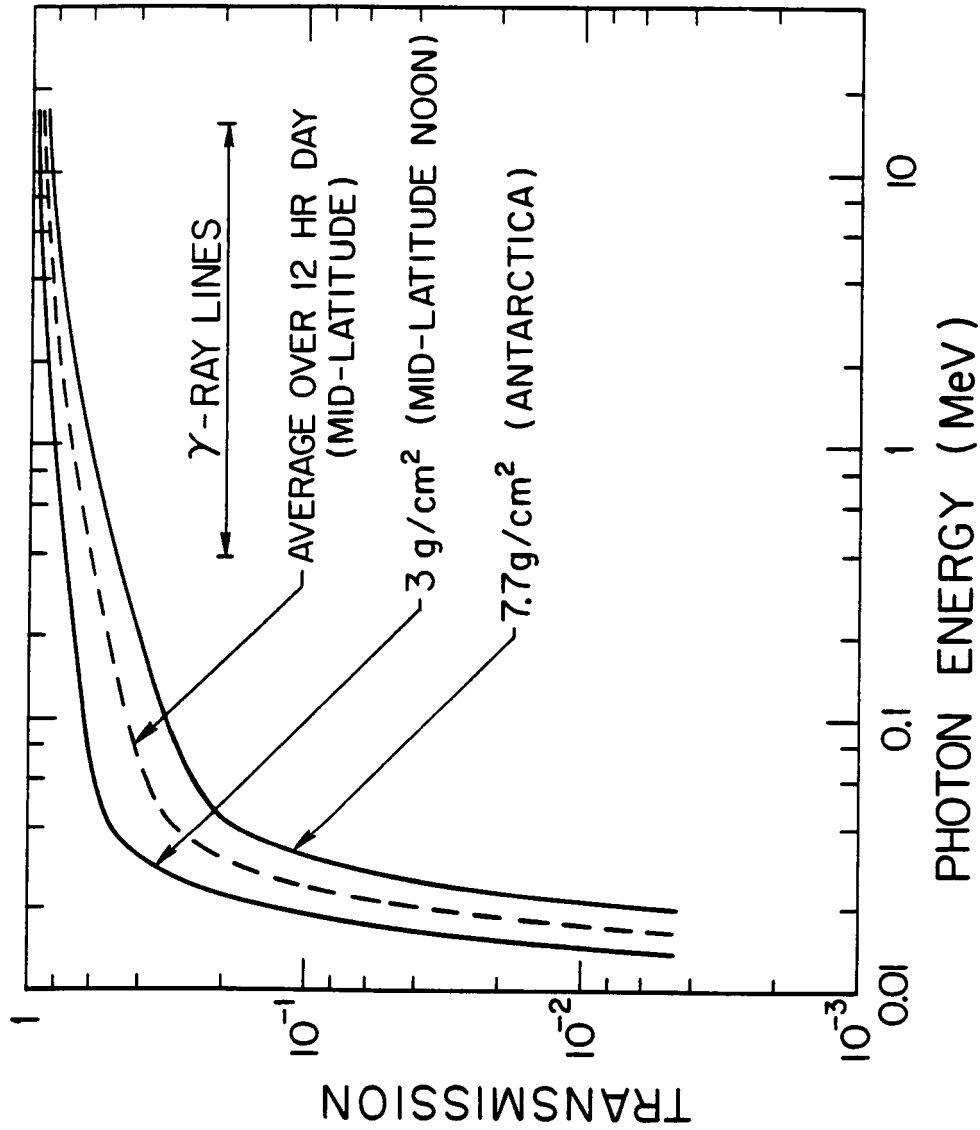


Fig. 7. Photon transmission for mid-latitudes (dashed line gives average over 12 hour day) as compared with Antarctica (24 hours/day).

Table III. HIREGS Event Probabilities*

	Mid-latitude 7 days (12 hrs/day)	Antarctica 12 days (24 hrs/day)
High resolution spectroscopy flare event ($>10\sigma$ in several lines)	~0.35	~1
Detection of several gamma-ray lines in a flare	1.4	~4
Detection of narrow 2.223 MeV neutron-capture line, if every flare accelerates >10 MeV ions	3.5	~10
Hard X-ray continuum fast spectroscopy flare (~1 sec detailed spectra)	14	~24
Hard X-ray microflares	≥ 700	~1200

* Assumes scaling with hard X-ray peak flux distribution measured by SMM.

Acknowledgments

This research was funded in part by NASA grants NAGW-516 and NAGW-449.

REFERENCES

1. R. Ramaty and R. E. Lingenfelter, *Ann. Rev. Nucl. Sci.* **32**, 235 (1982).
2. R. P. Lin and H. S. Hudson, *Solar Phys.* **50**, 153 (1976).
3. R. P. Lin, R. A. Schwartz, R. M. Pelling, and K. C. Hurley, *Astrophys. J. Lett.* **251**, L109 (1981).
4. R. P. Lin and R. A. Schwartz, *Astrophys. J.* **312**, 462 (1987).
5. E. L. Chupp, *Ann. Rev. Astron. Astrophys.* **22**, 359 (1984).
6. R. J. Murphy, R. Ramaty, D. J. Forrest, and B. Kozlovsky, *Proc. 19th Intern. Cosmic Ray Conf, La Jolla*, **4**, 240 and 253 (1985).
7. C. J. Crannell, G. Joyce, R. Ramaty, and C. Werntz, *Astrophys. J.* **210**, 582 (1976).
8. R. P. Lin, R. A. Schwartz, S. R. Kane, R. M. Pelling, and K. C. Hurley, *Astrophys. J.* **283**, 4211 (1984).
9. D. J. Forrest, W. T. Vestrand, E. L. Chupp, E. Rieger, J. Cooper, and G. Share, *19th Intern. Cosmic Ray Conf. Papers*, NASA Conf. Publ. 2376, Vol. 4 (NASA, Washington, D.C., 1985), p. 146.
10. P. N. Luke, *IEEE Trans. Nucl. Sci.* **NS-31**, 312 (1984).
11. J. L. Matteson, P. L. Nolan, W. D. Paciesas, and R. M. Pelling, *Space Sci. Instr.* **3**, 491 (1977).
12. D. A. Landis, F. S. Goulding, and R. M. Pehl, *IEEE Trans Nucl. Sci.* **NS-18**, 115 (1970).
13. D. J. Forrest, *Positron-Electron Pairs in Astrophysics*, M. L. Burns, A. K. Harding, and R. Ramaty, eds. (AIP, New York, 1983), p. 3.
14. D. J. Forrest, W. T. Vestrand, E. Rieger, and G. H. Share, *Bulletin American Astr. So.* **18**, 697 (1986).
15. J. Roth, J. H. Primbsch, and R. P. Lin, *IEEE Trans. Nucl. Sci.* **NS-31**, 367, 1984.
16. D. M. Smith, M. Shapshak, R. Campbell, J. H. Primbsch, and R. P. Lin, this volume (1988).
17. V. Lally, *Proc. XXIV COSPAR Conf., Ottawa, I*, 1.4 (1982).
18. R. Koga, F. M. Frye, Jr., A. Owen, B. V. Denehy, D. Mace, and J. Thomas, *19th Intern. Cosmic Ray Conf. Papers*, NASA Conf. Publ. 2376, Vol. 4 (NASA, Washington, D.C., 1985), p. 142.
19. R. P. Lin, D. W. Curtis, J. H. Primbsch, P. Harvey, W. K. Levedahl, D. M. Smith, R. M. Pelling, F. Duttweiler, and K. C. Hurley, *Solar Physics*, accepted for publication (1988).